Hydrogen-induced anomalies in the heat capacity of C15-type $ZrCr_2H_x$ $(ZrCr_2D_x)$

Hydrogen-induced anomalies in the heat capacity of C15-type $ZrCr_2H_x$ ($ZrCr_2D_x$)

A V Skripov, A E Karkin and A V Mirmelstein

Institute of Metal Physics, Urals Branch of the Academy of Sciences, Ekaterinburg 620219, Russia

Abstract.   Heat capacities $C(T)$ of C15-type $ZrCr_2H_x$ ($ZrCr_2D_x$) ($0 \leqslant x \leqslant 0.50$) have been measured in the temperature range 5.3–293 K. For all H- (D-) doped samples the low-temperature linear $C(T)$ term is found to contain considerable contributions of non-electronic origin. This feature is consistent with the existence of a glass-like low-energy excitation spectrum. The excess heat capacity strongly changes with hydrogen concentration, being nearly isotope independent. In the range 15–50 K marked deviations from the Debye behaviour of $C(T)$ are observed for all H- (D-) doped samples. In addition, for the samples with $x \geqslant 0.45$ the heat capacity shows a peak near 60 K which can be attributed to H (D) ordering.

1. Introduction

The behaviour of hydrogen in Laves phase compounds shows a number of interesting features including a rich variety of phase transitions [1], anomalous isotope effects [2, 3] and high H mobility down to low temperatures [4, 5]. The origin of the unusual hydrogen dynamics in these compounds is not yet clear. Measurements of the heat capacity are known to provide a sensitive probe of phase transitions and H excitations in metal–hydrogen systems [6, 7]. The aim of the present work is to study hydrogen-induced contributions to the heat capacity of the Laves phase compound $ZrCr_2$ with dissolved H and D.

$ZrCr_2$ may exist in the form of two structural modifications (the hexagonal C14 or the cubic C15) both of which absorb large amounts of hydrogen. Recent nuclear magnetic resonance (NMR) experiments [8–10] have revealed the anomalously high hydrogen mobility down to low temperatures in C15-type $ZrCr_2H_x$ ($x \leqslant 0.5$). The temperature dependence of the measured hydrogen diffusivity D in these compounds shows marked deviations from the Arrhenius behaviour below about 200 K [10]. Similar changes in the slope of Arrhenius plots of $D(T)$ suggesting changes in the diffusion mechanism have been found for α-NbH_x and α-TaH_x [11, 12]. The low-temperature hydrogen diffusion in these systems is believed to imply tunnelling of H between the ground states. It should be noted that high H mobility at low T in metal–hydrogen systems is often accompanied by anomalies in the hydrogen vibrational spectrum. Relevant examples are the α-phases of ScH_x, YH_x [13] and NbH_x [14].

No signs of a phase separation in C15-$ZrCr_2H_x$ with $x \leqslant 0.5$ have been found in NMR experiments [8, 9] down to 11 K; this is consistent with the tentative phase diagram of the $ZrCr_2$–H ($ZrCr_2$–D) system [1]. However, it is known that in some metal–hydrogen systems (e.g. in α-ScH_x and the related materials) the ordering of H (D) may provide the alternative to the decomposition, even at low H (D) concentrations [15]. Therefore, it is of interest to search for the effects of H (D) ordering in $ZrCr_2H_x$ ($ZrCr_2D_x$). Since the low-temperature motion of H (D) in $ZrCr_2H_x$ ($ZrCr_2D_x$) is likely to imply tunnelling, one

Table 1. Lattice parameters at room temperature and the limiting Debye temperatures for $ZrCr_2H_x$ ($ZrCr_2D_x$)

Sample	a (Å)	θ_D (K)
$ZrCr_2$	7.210	431 ± 7
$ZrCr_2H_{0.27}$	7.245	397 ± 5
$ZrCr_2D_{0.29}$	7.249	371 ± 8
$ZrCr_2H_{0.45}$	7.260	424 ± 7
$ZrCr_2D_{0.48}$	7.272	399 ± 7
$ZrCr_2H_{0.50}$	7.274	428 ± 6
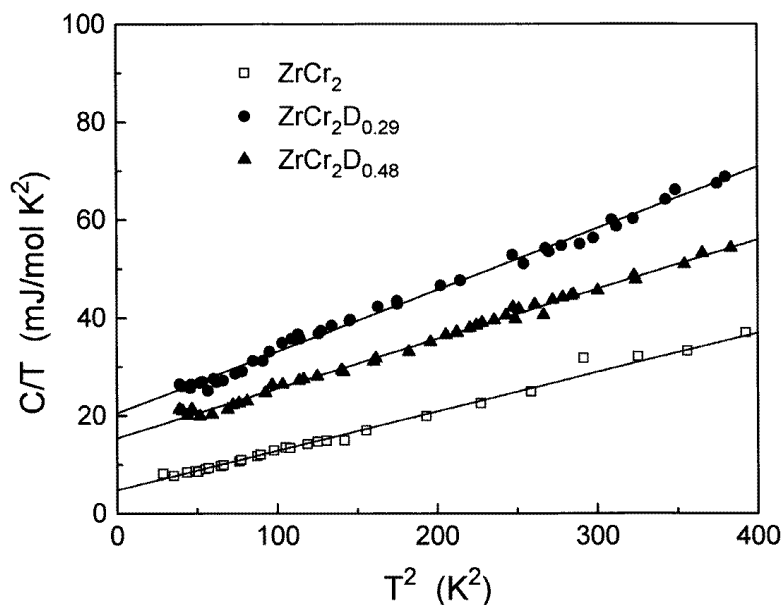
Figure 1. The low-temperature behaviour of C/T as a function of T^2 for $ZrCr_2$, $ZrCr_2D_{0.29}$ and $ZrCr_2D_{0.48}$. Solid lines represent least-squares fits of equation (1) to the data.

may also expect effects of hydrogen isotope substitution. In the present work we report the results of the heat capacity measurements of C15-type $ZrCr_2H_x$ ($ZrCr_2D_x$) with $0 \leqslant x \leqslant 0.5$ in the temperature range 5.3–293 K. For H-doped samples the experimental results have been partially published in our previous letter [16].

2. Experimental details

The $ZrCr_2$ alloy was prepared by arc melting the appropriate amounts of pure Zr and Cr in a helium atmosphere. The melting resulted in the formation of the hexagonal C14-type compound with the lattice parameters $a = 5.09$ Å and $c = 8.20$ Å. After the annealing in argon at 1300 °C for 3 h this sample was transformed into the single-phase cubic C15-type compound with $a = 7.210$ Å. All the hydrided and deuterided samples were prepared from the same ingot of $ZrCr_2$. Small pieces of $ZrCr_2$ were charged with H_2 gas at a pressure of about 0.3 bar using a Sieverts-type vacuum system, and the hydrogen content

was determined from the pressure change in the calibrated volume of the system. Heat capacity measurements were made on ZrCr$_2$H$_x$ samples with $x = 0$, 0.27, 0.45 and 0.50. After the measurements hydrogen was removed from ZrCr$_2$H$_{0.27}$ and ZrCr$_2$H$_{0.45}$ by heating in vacuum up to 800 °C, and deuterium was admitted into them, resulting in the compositions ZrCr$_2$D$_{0.29}$ and ZrCr$_2$D$_{0.48}$, respectively. This procedure should be important for the study of isotope (H↔D) effects in the heat capacity since the host material is exactly the same for the H- and D-doped compounds to be compared. NMR measurements did not find any traces of residual H atoms in the deuterided samples.

According to the x-ray diffraction analysis, all of the samples studied are single-phase compounds having the C15-type host lattice structure; their lattice parameters are listed in table 1. The heat capacity C was measured by the standard adiabatic method. Germanium and platinum resistance thermometers were used to measure the temperature in the ranges 5.3–20 K and 20–293 K, respectively. Experiments on the copper reference sample have shown that the accuracy of the heat capacity measurements is about 1–2% at $T \leqslant 7$ K, 0.5% between 7 and 15 K, and 0.4% in the range 15–293 K.
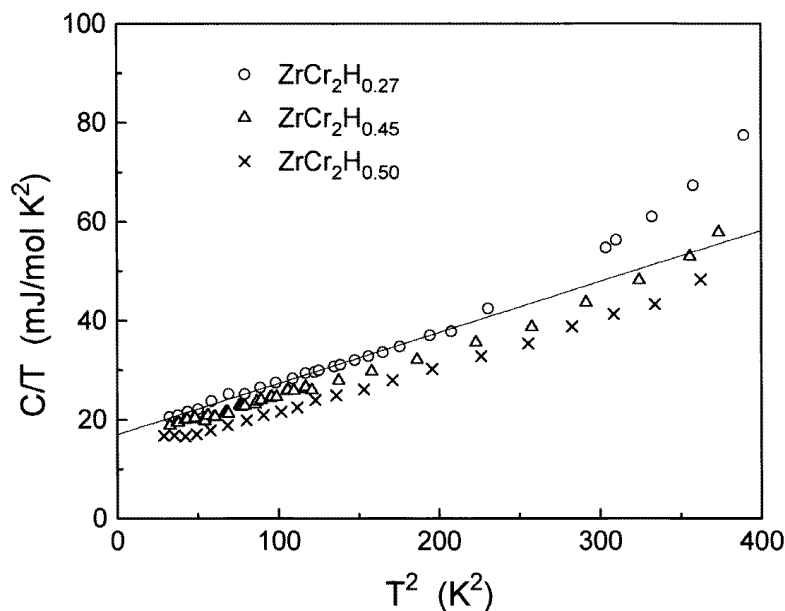

Figure 2. The low-temperature behaviour of C/T as a function of T^2 for ZrCr$_2$H$_{0.27}$, ZrCr$_2$H$_{0.45}$ and ZrCr$_2$H$_{0.50}$. The solid line represents the least-squares fit of equation (1) to the data for ZrCr$_2$H$_{0.27}$ below 15 K.

3. Results

The low-temperature behaviour of the heat capacity of ZrCr$_2$H$_x$ (ZrCr$_2$D$_x$) is shown in figures 1 and 2 in the usual C/T versus T^2 representation. The experimental data below 15 K (or below 20 K for some of the samples) can be described by the expression

$$C = \gamma T + \beta T^3. \tag{1}$$
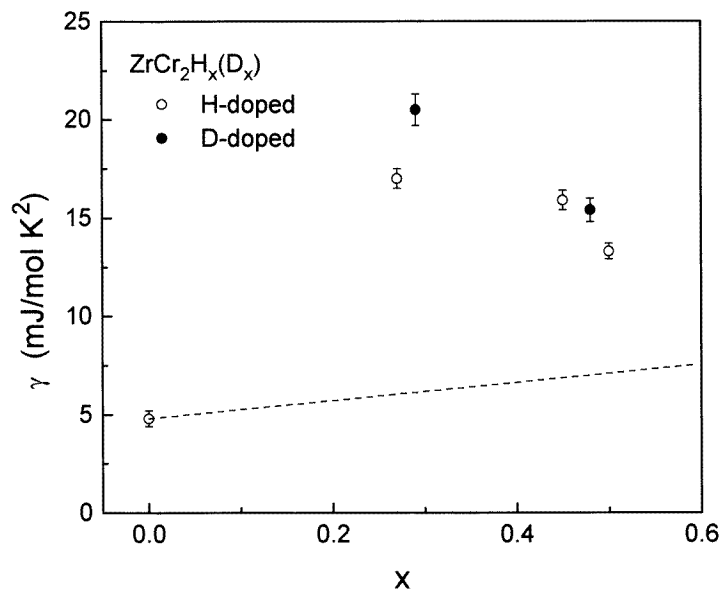
Figure 3. The value of γ as a function of H (D) content. The dashed line shows the expected behaviour of γ on the basis of $N(E_F)$ estimates.

In metals γ is usually identified as the electronic specific heat coefficient proportional to the density of electron states at the Fermi level, $N(E_F)$, and

$$\beta = (12/5)\pi^4 R z \theta_D^{-3} \tag{2}$$

with R, z and θ_D being the gas constant, the number of atoms per formula unit and the limiting Debye temperature, respectively. The values of γ and θ_D resulting from the least-squares fit of equation (1) to the data are presented in figure 3 and table 1, respectively. As can be seen from figure 3, the values of γ for H-doped and D-doped samples with nearly the same x are close to each other. However, the concentration dependence of γ appears to be non-monotonic. The most unusual feature is the strong difference between the apparent γ-values for the hydrogen-free and H- (D-) doped samples.

Figures 4 and 5 show the temperature dependence of C/T for $ZrCr_2H_x$ ($ZrCr_2D_x$) over the entire T-range studied. For the hydrogen-free $ZrCr_2$ the behaviour of C/T is that typical of crystalline solids. In contrast, for the H- (D-) doped samples strong deviations from the Debye behaviour of the heat capacity are observed. For all H- (D-) doped samples the value of C/T increases rapidly above 16–20 K and shows a shoulder-like feature near 30–40 K. The shoulder-like anomaly is pronounced more clearly for the samples with low x, being smeared out for $ZrCr_2H_{0.50}$. Figure 6 shows the temperature dependence of $(C-\gamma T)/T^3$ for four samples between 9 and 60 K. These axes are convenient for the analysis of deviations from the Debye behaviour of $C(T)$. As can be seen from figure 6, the effects of H (D) doping are dramatic. For the hydrogen-free $ZrCr_2$ the value of $(C - \gamma T)/T^3$ is nearly constant, as expected, whereas for the H- (D-) doped samples it shows a marked maximum.

An additional $C(T)$ feature is observed for the samples with $x \geqslant 0.45$ in the range 60–70 K. As can be seen from figures 4 and 5, in this range there is a distinct $C(T)$ peak for $ZrCr_2H_{0.45}$, $ZrCr_2D_{0.48}$ and $ZrCr_2H_{0.50}$. This peak may be attributed to some kind of H (D) ordering. Note that this feature is absent for the samples with lower x.
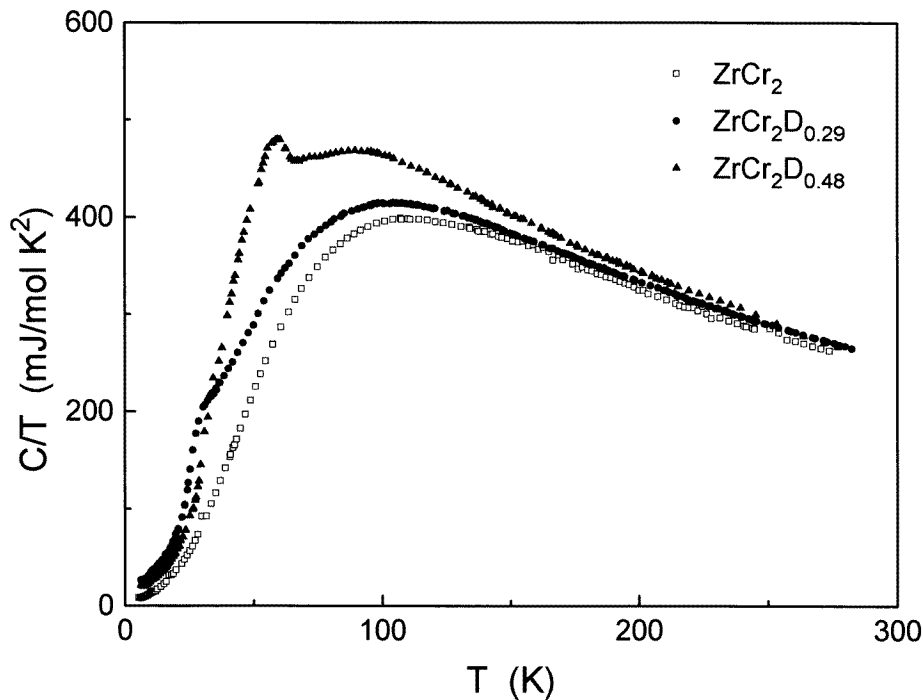
Figure 4. The temperature dependence of C/T for ZrCr$_2$, ZrCr$_2$D$_{0.29}$ and ZrCr$_2$D$_{0.48}$.

4. Discussion

4.1. $T \leqslant 15$ K

The non-monotonic dependence of γ on H (D) content and the strong difference between γ-values for the hydrogen-free and H- (D-) doped samples suggest the presence of considerable non-electronic contributions to the apparent γ-values. In fact, measurements of the magnetic susceptibility, the proton Knight shift and the electronic contribution to the proton spin–lattice relaxation rate [8, 9] unambiguously show that $N(E_F)$ in ZrCr$_2$H$_x$ increases monotonically with increasing x, and there are no sharp changes in $N(E_F)$ at $x \leqslant 0.5$. This is also consistent with the results of the x-ray photoelectron spectroscopy [17] and the band-structure calculations [18]. Similar behaviour of $N(E_F)$ as a function of x is observed for the related isoelectronic system TiCr$_2$H$_x$ [19]. Thus the observed H (D) concentration dependence of γ in ZrCr$_2$H$_x$ qualitatively differs from that of $N(E_F)$ (see figure 3).

The linear (or nearly linear) contributions to $C(T)$ of non-electronic origin are known to exist in glasses [20]. They can be accounted for by the two-level system (TLS) model [21] with a nearly uniform distribution of the energy gap values ΔE at low ΔE. However, the microscopic description of TLS in glasses remains to be elucidated. It is generally assumed that the existence of TLS in glasses is due to the disorder, so that a rearrangement of a group of atoms can switch the system between adjacent local energy minima. For a metal–hydrogen system it is natural to relate TLS with the motion of a *single* H atom in
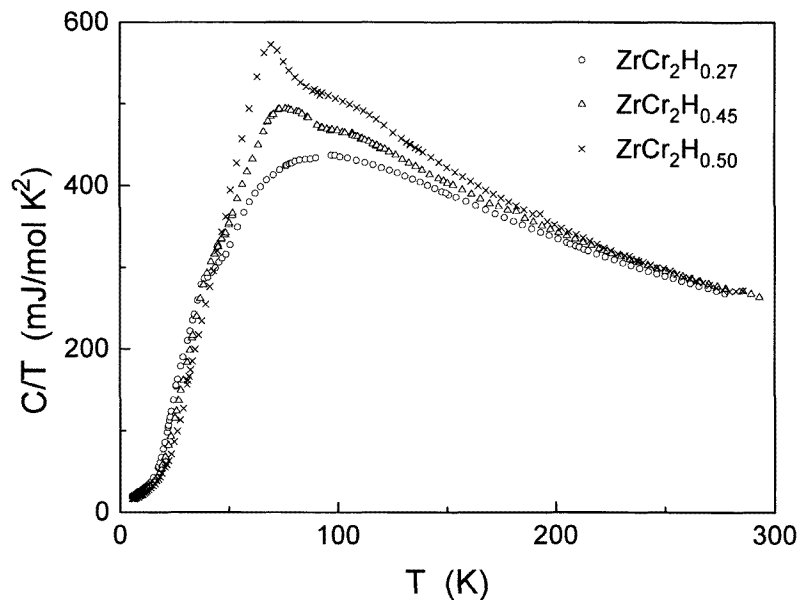
Figure 5. The temperature dependence of C/T for $ZrCr_2H_{0.27}$, $ZrCr_2H_{0.45}$ and $ZrCr_2H_{0.50}$.
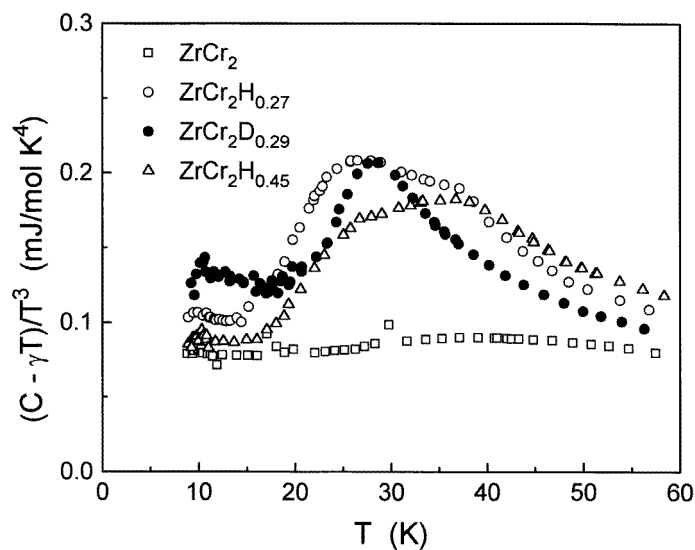
Figure 6. The temperature dependence of $(C - \gamma T)/T^3$ in the range 9–60 K.

a double-well potential. The relevant example is the tunnelling of hydrogen trapped by defects in niobium [22]. Neumaier *et al* [7] observed the excess low-temperature specific heat in $NbTi_{0.05}$ alloy doped with H and D (up to 3 at.%). This excess specific heat was found to be roughly proportional to temperature and H (D) content. Since Ti atoms in Nb act as trap centres for H (D), the observed effects were ascribed to hydrogen tunnelling

involving two or more interstitial sites near a Ti atom [7]. Recently the fast localized H motion that appears to be *intrinsic* (i.e. not related to hydrogen trapped by defects) has been found in two classes of metal–hydrogen systems: α-ScH$_x$ and the related materials [13, 23, 24] and C15-type TaV$_2$H$_x$ (TaV$_2$D$_x$) [4, 5, 25].

It is interesting to compare the excess specific heat values C_{exc} for NbTi$_{0.05}$H$_x$ (NbTi$_{0.05}$D$_x$) and for our ZrCr$_2$H$_x$ (ZrCr$_2$D$_x$) samples. In order to allow for different H (D) concentrations, we shall calculate C_{exc} for one H (D) atom per formula unit (i.e. for $x = 1$). Using the data of reference [7], we estimate the corresponding typical C_{exc}/T value for hydrogen-doped NbTi$_{0.05}$ to be 58 mJ mol^{-1} K^{-2}. Assuming that the electronic contribution to γ for ZrCr$_2$H$_{0.27}$ is 6 mJ mol^{-1} K^{-2} (i.e. about 25% higher than for ZrCr$_2$, in accordance with $N(E_{\text{F}})$ estimates), we obtain for this compound $C_{\text{exc}}/T \approx 41$ mJ mol^{-1} K^{-2}, as scaled to $x = 1$. Thus the values of the excess specific heat per H (D) atom in NbTi$_{0.05}$H$_x$ (NbTi$_{0.05}$D$_x$) and ZrCr$_2$H$_x$ (ZrCr$_2$D$_x$) are of the same order of magnitude. This is consistent with the description of C_{exc} in ZrCr$_2$H$_x$ (ZrCr$_2$D$_x$) in terms of two-level systems each of which is related to the motion of a single H (D) atom.

We now turn to discussion of the unusual dependence of C_{exc} in ZrCr$_2$H$_x$ (ZrCr$_2$D$_x$) on H (D) content. For non-interacting systems of H (D) atoms one would expect the linear concentration dependence of C_{exc}. This behaviour was observed for NbTi$_{0.05}$H$_x$ (NbTi$_{0.05}$D$_x$) in the range of very small H (D) concentrations. However, as the hydrogen concentration increases, interactions between H (D) atoms may lead to the formation of ordered atomic configurations where the fast H (D) motion is suppressed. The decrease in the fraction of H atoms participating in the fast localized motion with increasing x has been found, for example, in α-ScH$_x$, and is explained by the growth of a number of stable pairs of H atoms along the c-axis [13]. Therefore the observed maximum of C_{exc} as a function of x can result from the competition between the increasing total number of H (D) atoms and the decreasing fraction of atoms participating in the localized motion. The evidence for H (D) ordering in ZrCr$_2$H$_x$ (ZrCr$_2$D$_x$) will be discussed in the next section.

As in the case of NbTi$_{0.05}$H$_x$ (NbTi$_{0.05}$D$_x$) [7], we have not observed any pronounced difference between C_{exc}-values for H- and D-doped samples with nearly the same H (D) content. The plausible explanation of this fact in terms of the TLS model implies that the tunnelling matrix elements for both H and D are smaller than the lowest excitation energy probed in our experiments ($\sim$1 meV). In this case the observed excitation spectrum is determined by the asymmetry of the double-well potential which is expected to be isotope independent.

4.2. $15 \leqslant T \leqslant 100$ K

The observed maximum of $(C - \gamma T)/T^3$ as a function of T for H- and D-doped samples (see figure 6) suggests the presence of additional hydrogen-induced vibrational modes within the low-frequency (acoustic) part of the vibrational spectrum. Note that similar maxima in C/T^3 near 10–20 K are typical of glasses [20]; they may be ascribed to the soft quasilocalized vibrational modes [26]. A rough estimate of the density of such additional modes n can be obtained by comparing the energy of a single mode with the total excess vibrational energy. The energy of the soft mode is expected to be of the order of $4.9k_{\text{B}}T_{\text{max}}$ [27], where T_{max} is the temperature of the $(C - \gamma T)/T^3$ maximum. The total excess vibrational energy can be estimated from the heat capacity data by subtracting the Debye contribution and integrating over the temperature range of the anomaly. For ZrCr$_2$H$_{0.27}$ such an estimate in the range 15–50 K gives $n = 0.1$ (per formula unit). This value is of the same order of magnitude as the hydrogen concentration ($x = 0.27$) in the sample.

The microscopic origin of the soft quasilocalized vibrational modes in glasses is not yet clear. However, model calculations [26] show that these modes may originate from some 'defect' regions, i.e. the regions with the local structure strongly differing from that of the 'average' glass. Therefore, the concept of the soft quasilocalized modes appears to be close to that of the resonant modes known in the phonon theory of defects in crystals [28]. Taking into account the above estimate of the mode density, it seems reasonable to ascribe the anomalies in $C(T)$ for $ZrCr_2H_x$ ($ZrCr_2D_x$) near 30 K to the low-frequency resonant modes of H (D). Such low-frequency resonant vibrations have been earlier found for hydrogen in $NbH_{0.05}$ [14] and $LaNi_5H_6$ ($LaNi_5D_6$) [29] by means of inelastic neutron scattering; they give rise to sharp peaks in the vibrational spectrum near 16 meV and 12 meV, respectively. It would be interesting to look for a similar peak in the vibrational spectrum of $ZrCr_2H_x$ ($ZrCr_2D_x$). To the best of our knowledge, no neutron spectroscopic studies of $ZrCr_2H_x$ ($ZrCr_2D_x$) have been reported so far. Comparison of the $(C - \gamma T)/T^3$ data for $ZrCr_2H_{0.27}$ and $ZrCr_2D_{0.29}$ (figure 6) shows only minor effects of hydrogen isotope substitution on T_{max}. Note that for $LaNi_5H_6$ ($LaNi_5D_6$) the energy of the low-frequency resonant mode was also found to be isotope independent [29].
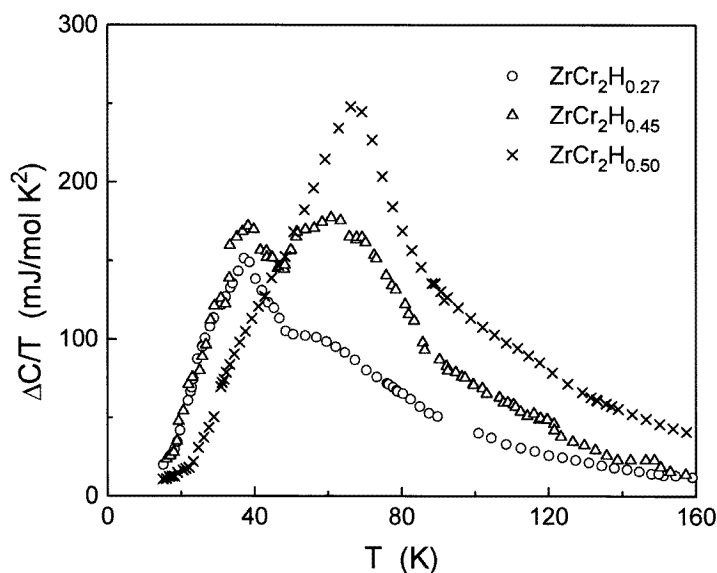
Figure 7. The temperature dependence of $\Delta C/T$, where ΔC is the excess heat capacity, for three H-doped samples in the range 15–160 K.

The C/T peak observed for the samples with $x \geqslant 0.45$ in the range 60–70 K is likely to result from H (D) ordering. This is consistent with the tentative phase diagram of $ZrCr_2$–H ($ZrCr_2$–D) [1]. The low-x part of this diagram is based on the observation of superstructure lines in the low-temperature neutron diffraction pattern of C15-type $ZrCr_2D_{0.7}$. Similar peaks in C/T have been found in the related C15-type system TaV_2H_x (TaV_2D_x) in the range 70–110 K [30], and the subsequent neutron diffraction measurements [31] have confirmed that these peaks originate from H (D) ordering. The dependence of $C(T)$ on H (D) concentration in $ZrCr_2H_x$ ($ZrCr_2D_x$) is also consistent with H (D) ordering near 70 K. Figure 7 shows the behaviour of the excess heat capacity ΔC defined as the difference between the value of C for a H-doped sample and the smoothed data for the hydrogen-free $ZrCr_2$. For the sake

of clarity the data for D-doped samples are omitted. It can be seen that the $\Delta C/T$ peak near 70 K increases with increasing x, as expected for hydrogen ordering. On the other hand, the feature near 30 K becomes less pronounced at higher x. Thus the tendency to H (D) ordering seems to suppress the contribution due to the resonant mode. The $\Delta C/T$ maximum for ZrCr$_2$D$_{0.48}$ is observed at 55 K, whereas the temperatures of the corresponding maxima for ZrCr$_2$H$_{0.45}$ and ZrCr$_2$H$_{0.50}$ are 61 and 66 K, respectively. Hence the ordering temperature for D appears to be somewhat lower than for H. The sign of this isotope effect is opposite to that found for TaV$_2$H$_x$ (TaV$_2$D$_x$) [30]. For both ZrCr$_2$H$_x$ (ZrCr$_2$D$_x$) and TaV$_2$H$_x$ (TaV$_2$D$_x$) the nature of the isotope effects in the ordering temperature and the low-temperature ordered structures remain to be elucidated.

4.3. $T \geqslant 100$ K

In this temperature range the heat capacity of H- (D-) doped samples is expected to contain contributions due to the high-frequency (optical) vibrations of hydrogen or deuterium. Such contributions are present in our experimental data. Assuming that these contributions are described by the Einstein formula, we can estimate the characteristic Einstein temperature θ_E from the data. The corresponding estimates for ZrCr$_2$H$_{0.45}$ and ZrCr$_2$D$_{0.48}$ lead to the θ_E-values of 1290 K and 1030 K, respectively. As expected, these values show the isotope effect, being consistent with typical energies of the optical vibrations of hydrogen in metals ($\sim$100 meV). However, these values should be considered only as rough estimates, since the upper limit of our experimental temperature range is not high enough for probing the optical vibrations of hydrogen.

5. Conclusions

Our measurements have revealed a number of hydrogen-induced anomalies in the heat capacity of C15-type ZrCr$_2$H$_x$ (ZrCr$_2$D$_x$) with $x \leqslant 0.5$.

(1) The low-temperature linear $C(T)$ term for H- (D-) doped samples is found to contain considerable contributions of non-electronic origin. This glass-like feature may be interpreted in terms of the tunnelling two-level systems each of which is related to the motion of a single H (D) atom. Interactions between H (D) atoms are expected to reduce the number of such tunnelling two-level systems at high H (D) concentrations.

(2) The heat capacity of H- (D-) doped samples shows strong deviations from the Debye behaviour in the range 15–50 K. The manifestation of these deviations is the marked maximum of $(C - \gamma T)/T^3$ near 30 K. The observed behaviour of $C(T)$ in this range may be ascribed to the low-frequency localized vibrations of hydrogen (resonant modes).

(3) For the samples with $x \geqslant 0.45$ the additional $C(T)$ peak is found in the range 60–70 K. This peak is attributed to H (D) ordering.

It is interesting to note that the C15-type ZrCr$_2$H$_x$ (ZrCr$_2$D$_x$) system exhibits a combination of the high hydrogen mobility down to low temperatures, the low-frequency anomalies in the hydrogen vibrational spectrum and the low-T hydrogen ordering. These properties may be related to each other. In fact, similar relations between the hydrogen ordering and the unusual local hydrogen dynamics have been discussed for α-ScH$_x$ [13] and C15-type TaV$_2$H$_x$ (TaV$_2$D$_x$) [25]. The microscopic picture of both H (D) ordering and dynamics in ZrCr$_2$H$_x$ (ZrCr$_2$D$_x$) may be clarified by neutron scattering experiments. Such experiments are in progress now.

References

[1] Somenkov V A and Irodova A V 1984 *J. Less-Common Met.* **101** 481
[2] Skripov A V, Belyaev M Yu, Kozhanov V N, Stepanov A P, Kost M E and Padurets L N 1986 *Solid State Commun.* **57** 249
[3] Skripov A V, Belyaev M Yu, Rychkova S V and Stepanov A P 1991 *J. Phys.: Condens. Matter* **3** 6277
[4] Skripov A V, Belyaev M Yu, Rychkova S V and Stepanov A P 1989 *J. Phys.: Condens. Matter* **1** 2121
[5] Skripov A V, Rychkova S V, Belyaev M Yu and Stepanov A P 1990 *J. Phys.: Condens. Matter* **2** 7195
[6] Nace D M and Aston J G 1957 *J. Am. Chem. Soc.* **79** 3623
[7] Neumaier K, Wipf H, Cannelli G and Cantelli R 1982 *Phys. Rev. Lett.* **49** 1423
[8] Skripov A V, Belyaev M Yu and Stepanov A P 1991 *Solid State Commun.* **78** 909
[9] Skripov A V and Belyaev M Yu 1993 *J. Phys.: Condens. Matter* **5** 4767
[10] Renz W, Majer G, Skripov A V and Seeger A 1994 *J. Phys.: Condens. Matter* **6** 6367
[11] Völkl J and Alefeld G 1978 *Hydrogen in Metals I* ed G Alefeld and J Völkl (Berlin: Springer) p 321
[12] Hampele M, Majer G, Messer R and Seeger A 1991 *J. Less-Common Met.* **172–174** 631
[13] Berk N F, Rush J J, Udovic T J and Anderson I S 1991 *J. Less-Common Met.* **172–174** 496
[14] Lottner V, Schober H R and Fitzgerald W J 1979 *Phys. Rev. Lett.* **42** 1162
[15] Blaschko O 1991 *J. Less-Common Met.* **172–174** 237
[16] Skripov A V and Mirmelstein A V 1993 *J. Phys.: Condens. Matter* **5** L619
[17] Schlapbach L, Osterwalder J and Riesterer T 1984 *J. Less-Common Met.* **103** 295
[18] Gupta M and Schlapbach L 1988 *Hydrogen in Intermetallic Compounds I* ed L Schlapbach (Berlin: Springer) p 139
[19] Bowman R C, Lynch J F and Johnson J R 1982 *Mater. Lett.* **1** 122
[20] Hunklinger S and Raychaudhuri A K 1986 *Prog. Low Temp. Phys.* **9** 267
[21] Phillips W A 1987 *Rep. Prog. Phys.* **50** 1657
[22] Wipf H, Steinbinder D, Neumaier K, Gutsmiedl P, Magerl A and Dianoux A J 1987 *Europhys. Lett.* **4** 1379
[23] Lichty L R, Han J W, Ibanez-Meier R, Torgeson D R, Barnes R G, Seymour E F W and Sholl C A 1989 *Phys. Rev.* B **39** 2012
[24] Svare I, Torgeson D R and Borsa F 1991 *Phys. Rev.* B **43** 7448
[25] Skripov A V, Cook J C, Karmonik C and Hempelmann R 1996 *J. Phys.: Condens. Matter* **8** L319
[26] Schober H R and Laird B B 1991 *Phys. Rev.* B **44** 6746
[27] Junod A 1980 *Solid State Commun* **33** 55
[28] Maradudin A A, Montroll E W, Weiss G H and Ipatova I P 1971 *Theory of Lattice Dynamics in the Harmonic Approximation (Solid State Physics Suppl. 3)* (New York: Academic)
[29] Bührer W, Furrer A, Hälg W and Schlapbach L 1979 *J. Phys. F: Met. Phys.* **9** L141
[30] Skripov A V, Mirmelshtein A V and Belyaev M Yu 1992 *Solid State Commun.* **81** 689
[31] Fischer P, Fauth F, Skripov A V, Podlesnyak A A, Padurets L N, Shilov A L and Ouladdiaf B 1997 *J. Alloys Compounds* at press